Doping studies of the magnetic cobaltocuprate $CoSr_2Y_{2-x}Ce_xCu_2O_{9\pm\delta}$

Abbie Christina Mclaughlin[a],*, David Morrice[a], Falak Sher[b]

[a]Chemistry Department, University of Aberdeen, Meston Walk, Aberdeen, AB24 3UE, UK
[b]Centre for Science at Extreme Conditions and School of Chemistry, University of Edinburgh, Kings's Buildings, West Mains Road, Edinburgh, EH9 3JZ, UK

Abstract

A structural, magnetic and electronic study of the cobaltocuprate $CoSr_2Y_{2-x}Ce_xCu_2O_{9\pm\delta}$ ($x = 0.5-0.8$) has been performed. All materials crystallise in the orthorhombic $Cmcm$ symmetry space group in which chains of corner linked CoO_4 tetrahedra run parallel to the 110 direction. An antiferromagnetic transition is observed for $x = 0.5-0.8$; T_M increases with x. A change in the dimensionality of the magnetic order occurs at $x = 0.8$ as the interchain distance increases to a critical value. There is charge transfer between the cuprate planes and cobaltate layer as Ce doping increases, so that Co^{3+} is partially oxidised to Co^{4+} with a concomitant reduction in the valence of Cu. Superconductivity is not observed in any of the samples and a crossover from Mott to Efros and Shklovskii variable range hopping behaviour is evidenced as x increases from 0.5 to 0.8.
© 2005 Elsevier Inc. All rights reserved.

Keywords: Antiferromagnetism; Superconductivity; $RuSr_2GdCu_2O_8$; Triple perovskite; Spin glass

1. Introduction

The coexistence of weak ferromagnetism and superconductivity has recently been observed in the layered ruthenocuprates $RuSr_2GdCu_2O_8$ (1212) and $RuSr_2RE$ $CeCu_2O_{10}$ (1222) (RE = Gd, Eu, Sm) [1–11]. In both these materials the superconductivity occurs in the CuO_2 planes ($T_c = 0-37$ K depending upon sample preparation) and the weak ferromagnetism in the RuO_2 layer ($T_M = 125-215$ K). μSR experiments have demonstrated that the materials are microscopically uniform with no evidence of spatial phase separation of superconducting and magnetic regions [3]. Neutron scattering experiments on $RuSr_2GdCu_2O_8$ have recently shown that G-type antiferromagnetic order is present within the RuO_2 planes [6]. An upper limit of $0.1\mu_B$ was obtained for the ferromagnetic component. Upon

application of a magnetic field the Ru spins cant further away from the G-type magnetic structure and at 7 T the order of the Ru spins is fully ferromagnetic. It is thought that the weak ferromagnetism arises via a canting of the Ru spins in both $RuSr_2GdCu_2O_8$ and $RuSr_2RECe$ Cu_2O_{10}. This occurs due to the antisymmetric Dzyaloshinsky-Moriya interaction between neighbouring Ru moments, [12,13] which is non-zero due to the tilts and rotations of the RuO_6 octahedra observed in synchrotron X-ray and neutron diffraction studies [4,5]. Recent neutron and synchrotron X-ray powder diffraction studies have shown that rotations and tilts of the RuO_6 octahedra also occur in $Gd_{1.3}Ce_{0.7}RuSr_2Cu_2O_{10}$ [7,8].

Since the discovery of weak ferromagnetism and superconductivity in the ruthenocuprates it has been proposed that the coexistence of the usually antagonistic phenomena of ferromagnetism and superconductivity could be possible if the superconducting and ferromagnetic subsystems are disjoint and a Fulde-Ferrell-

*Corresponding author. Fax: +44 1224 272921.
E-mail address: a.c.mclaughlin@abdn.ac.uk (A.C. Mclaughlin).

Larkin-Ovchinnikov-type state [9], a self-induced vortex state [10] or a crypto-superconducting structure [11] occurs. In an attempt to observe coexisting super-conductivity and ferromagnetic order $CoSr_2Y_{2-x}Ce_x Cu_2O_{9\pm\delta}$ has been studied. Interesting magnetic behaviour has been observed recently in cobalt oxides; $Sr_2Y_{0.5}Ca_{0.5}Co_2O_7$ exhibits ferromagnetic behaviour with a coulomb gap [14]; magnetoresistance is observed in the compounds $La_{1-x}Sr_xCoO_3$ [15] and $YBaCo_2O_5$ [16]. Hence $CoSr_2Y_{2-x}Ce_xCu_2O_{9\pm\delta}$ is an attractive candidate to exhibit the phenomena of ferromagnetism and superconductivity.

$CoSr_2Y_{1.5}Ce_{0.5}Cu_2O_{9\pm\delta}$ is not superconducting [17] but a recent study has shown that magnetic order is present in the cobaltate layer below $T_M = 40$ K [18,19]. The oxidation state of Ce is IV in these materials [18] so that the total formal charge for $(2Cu + Co)$ is $7.5 \pm 2\delta$, where δ is equal to the oxygen deficiency or excess in the $Y_{1.5}Ce_{0.5}O_{2\pm\delta}$ block. It has previously been reported that oxygen vacancies in $Gd_{2-x}Ce_xRuSr_2Cu_2O_{10-\delta}$ are located on the O(4) site within the $Gd_{2-x}Ce_xO_2$ block [8]. The magnetic and superconducting transitions can be controlled simultaneously by varying the Gd/Ce ratio in $RuSr_2Gd_{2-x}Ce_xCu_2O_{10-\delta}$ [8]. Substitution of Ce^{4+} for Gd^{3+} at constant oxygen content would lead to a reduction in the hole-doping of the copper or ruthenium layers. However, since in the 1222 structure the two $(Gd_{1-x/2}Ce_{x/2})$ layers sandwich a defective oxygen layer, the increase in the cation layer charge with x can be charge-compensated by an increase of the oxygen content. As x is increased in the $RuSr_2Gd_{2-x}Ce_xCu_2O_{10-\delta}$ solid solutions there is actually an over-compensating increase in oxygen so that an overall increase in hole doping of the CuO_2 layers arises and T_c increases from 0 to 30 K as x increases from 0.5 to 0.7. At the same time the magnetic transition temperature increases from 151 to 165 K. In an attempt to induce superconductivity in $CoSr_2Y_{2-x}Ce_xCu_2O_{9\pm\delta}$, solid solutions with $x = 0.5$, 0.6, 0.7, 0.8 have been prepared and the structural, magnetic and electrical properties of this cobaltocuprate have been studied.

2. Experimental

Ceramic $CoSr_2Y_{2-x}Ce_xCu_2O_{9\pm\delta}$ samples ($x = 0.5$, 0.6, 0.7, 0.8) were prepared by the solid-state reaction of the stoichiometric oxides Y_2O_3, CeO_2, $SrCO_3$, Co_3O_4 and CuO. These were ground, die-pressed into pellets and preheated for 10 h at 1000 °C. The samples were reground, repelleted and sintered at 1100 °C for 30 h under flowing oxygen and then furnace cooled to ambient temperature.

Room temperature X-ray diffraction patterns were collected for the $CoSr_2Y_{2-x}Ce_xCu_2O_{9\pm\delta}$ solid solutions on a Bruker D8 Advance diffractometer with twin

Gobel mirrors using $CuK\alpha_1$ radiation. Data were collected over the range $5° < 2\theta < 100°$, with a step size of 0.02°.

Magnetisations were measured between 10 and 300 K on a Quantum Design SQUID magnetometer in an applied field of 0.1 T after zero-field (ZFC) and field cooling (FC). Variable field magnetisation data were recorded at 10 K for all samples with the field swept between ± 10 kOe. The resistivities of sintered poly-crystalline bars were measured between 6 and 350 K using the standard four-probe dc technique on a Quantum Design physical properties measurement system (PPMS). The oxygen content of the samples was determined by thermogravimetric analysis in a 5% H_2/N_2 atmosphere using a Stanton Redcroft 780 thermal analyser. Data were recorded at a rate of 5 °C/min between temperatures of 20–850 °C; under such conditions the $CoSr_2Y_{2-x}Ce_xCu_2O_{9\pm\delta}$ phases decomposed to a mixture of Cu, CoO, SrO, CeO_2 and Y_2O_3 in a single step between 300 and 750 °C.

3. Results

X-ray diffraction patterns demonstrated that the $CoSr_2Y_{2-x}Ce_xCu_2O_{9\pm\delta}$ solid solutions are phase pure. The X-ray diffraction data were all fitted by the Rietveld method [20] using the GSAS programme [21]. The backgrounds were fitted using linear interpolation and the peak shapes were modelled using a pseudo-Voigt function. An excellent Rietveld fit was obtained for all samples using the model previously reported for $CoSr_2Y_{1.5}Ce_{0.5}Cu_2O_{9\pm\delta}$ [17] (space group $Cmcm$, $a = 28.1548(7)$ Å, $b = 5.4255(1)$ Å, $c = 5.4013(1)$ Å) (Fig. 1). This structure contains Cu in square pyramidal geometry and chains of corner linked CoO_4 tetrahedra. Room
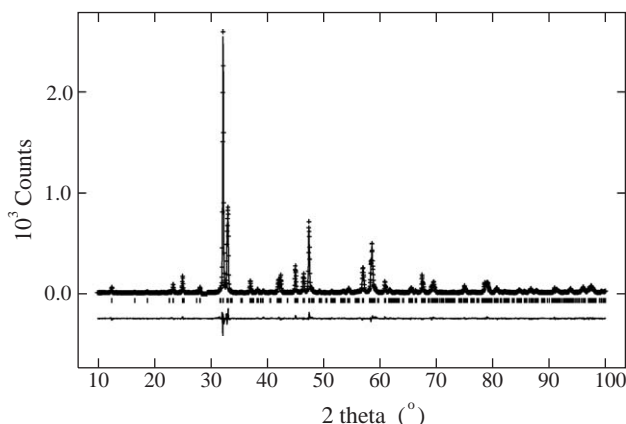

Fig. 1. Rietveld refinement fit to the powder X-ray diffraction pattern of $CoSr_2Y_{1.4}Ce_{0.6}Cu_2O_{9\pm\delta}$. Crosses are observed data and upper line the fitted profile to the $Cmcm$ symmetry structural model. The lower line shows the difference between the observed data and fitted model.

temperature neutron studies have shown that there is no intermixing of Co and Cu ions in the two different geometries [17]. The CoO_4 chains run parallel to the 1 1 0 direction leading to an enlarged orthorhombic superstructure and can link up in one of two ways (left, **L** or right, **R**); the **R** structure is shown in Fig. 2. In $CoSr_2Y_{1.5}Ce_{0.5}Cu_2O_{9\pm\delta}$ both types of chain are present in equal quantities, however chain directional order is preserved so that orthorhombic symmetry is observed. Recent results have suggested that $CoSr_2Y_{1.5}Ce_{0.5}Cu_2O_{9\pm\delta}$ crystallises in the tetragonal $I4/mmm$ symmetry model [18,19]. In this model there is no long-range directional ordering of the CoO_4 tetrahedra and hence tetragonal symmetry. An attempt was made to model the data using this space group, however a much improved fit is obtained when refining the data with the orthorhombic $Cmcm$ model described above ($\chi^2 = 1.05$ and 2.05; $R_{WP} = 7.81$ and 17.19; $R_P = 6.17$ and 13.62 for the $Cmcm$ and $I4/mmm$ symmetry models respectively).

As expected the a cell parameter decreases from 28.1548(6) to 28.1457(6) as the proportion of the smaller
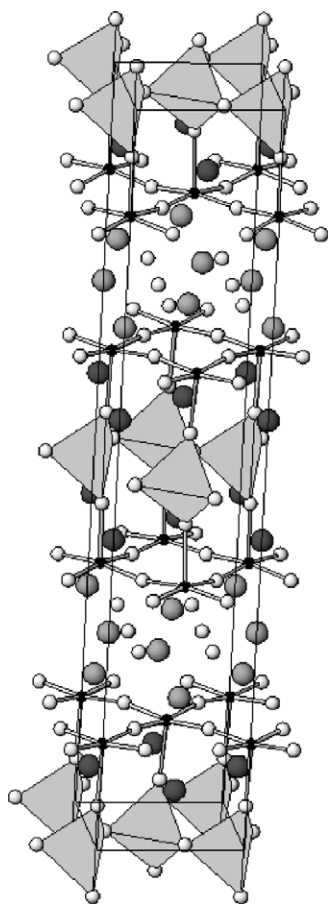
Ce^{4+} ion increases from 0.5 to 0.8. However the cell volume, b and c cell parameters all increase with x in the $CoSr_2Y_{2-x}Ce_xCu_2O_{9\pm\delta}$ solid solutions (Fig. 3). Furthermore there is an increase in both the apical Cu–O(1) and in plane Cu–O(2b) bonds from 2.295(9) and 1.901(4) to 2.322(9) and 1.923(4) respectively. At the same time the apical Co–O(1) and in plane Co–O(3) bonds decrease (Table 1).

Magnetic order is observed in all four samples (Fig. 4) at low temperature as previously reported for both $CoSr_2Y_{1.5}Ce_{0.5}Cu_2O_{9\pm\delta}$ and $CoSr_2Y_{0.6}Ca_{0.4}Cu_2O_7$ at approximately 40 K [19,22]. The magnetic transition temperature T_M was calculated from the derivative and increases from 43 to 67 K as x increases from 0.5 to 0.7 in the $CoSr_2Y_{2-x}Ce_xCu_2O_{9\pm\delta}$ solid solutions (Table 2). Divergence between the zero-field cooled (ZFC) and field cooled data (FC) is observed for $x = 0.5-0.7$ at the magnetic transition. This is suggestive of ferromagnetism, weak ferromagnetism (canted antiferromagnetism) or spin glass behaviour. Surprisingly there is no difference between the ZFC and FC magnetisation data for the $x = 0.8$ sample (Fig. 4). The magnetic transition becomes broader and weaker as x increases and at $x = 0.8$, a broad maximum around 128 K followed by an up-turn with decreasing temperature is observed. Similar behaviour has been reported for $Sr_2CoCuS_2O_2$ [23] and corresponds to low dimensional antiferromagnetic order. The high temperature data was fitted to the Curie Weiss law: $\chi_{mol} = \chi_0 + C/T - \theta$, where χ_0 and θ are the temperature independent susceptibility and Weiss constant respectively. The parameters χ_0, C and θ were determined by a least squares fit in the region 160 to 300 K. μ_{eff} increases from 5.12(2) to 5.46(2) and the Weiss constant decreases from −311 to −370 K (Table 2) as x increases from 0.5 to 0.8.

A superconducting transition was not observed in any of the samples; all samples display semiconducting behaviour. The resistivity was measured between 6 and

Fig. 2. The crystal structure of $CoSr_2Y_{2-x}Ce_xCu_2O_{9\pm\delta}$ (R) showing the corner linked CoO_4 chains. Open white circles, oxygen; small black circles, copper; large dark grey circles, strontium; large light grey circles, yttrium or cerium; tetrahedra, CoO_4.
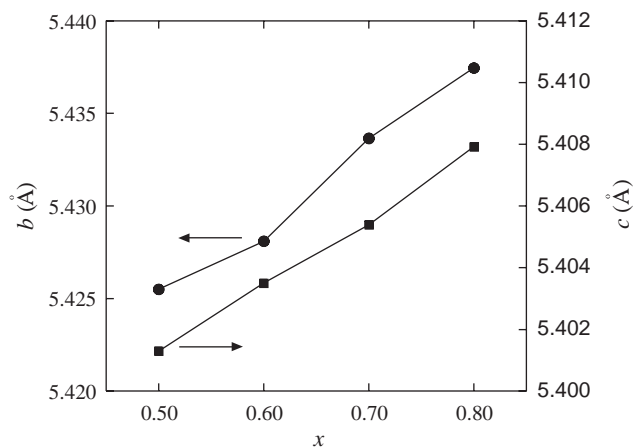
Fig. 3. Variation of the b and c cell parameters with x in the $CoSr_2Y_{2-x}Ce_xCu_2O_{9\pm\delta}$ solid solutions.

Table 1
Refined cell data, agreement factors, and selected bond lengths (Å) and angles (°)

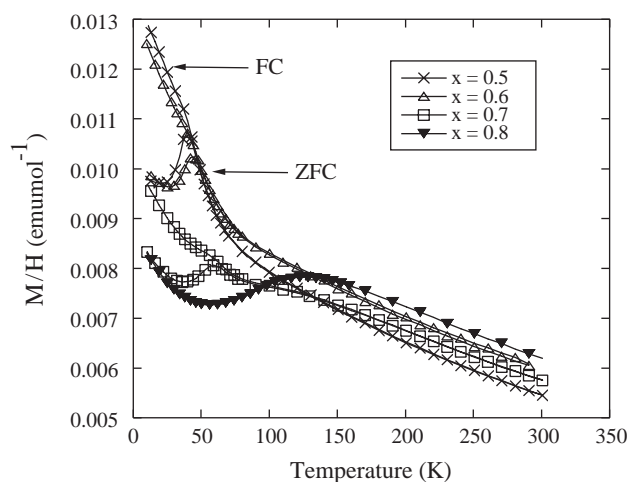|	0.5	0.6	0.7	0.8
a (Å)	28.1548(6)	28.1548(6)	28.1444(5)	28.1457(6)
b (Å)	5.4255(1)	5.4281(1)	5.4337(1)	5.4375(1)
c (Å)	5.4013(1)	5.4035(1)	5.4054(1)	5.4079(1)
V (Å^3)	825.06(4)	825.81(4)	826.63(4)	827.64(4)
χ^2	1.05	1.04	1.07	1.06
R_{WP} (%)	7.81	7.77	8.69	8.71
R_P (%)	6.17	6.09	6.71	6.70
Y/Ce–O(2a)	2.520(13)	2.516(13)	2.530(13)	2.519(13)
Y/Ce–O(2b)	2.477(11)	2.487(11)	2.475(11)	2.479(11)
Y/Ce–O(4)	2.303(13)	2.291(13)	2.309(13)	2.303(13)
Cu–O(1)	2.295(9)	2.317(9)	2.318(9)	2.322(9)
Cu–O(2a)	1.938(4)	1.935(4)	1.926(4)	1.934(4)
Cu–O(2b)	1.901(4)	1.906(4)	1.920(4)	1.923(4)
Co–O(1)	1.818(9)	1.802(9)	1.787(9)	1.796(9)
Co–O(3a)	2.115(14)	2.175(14)	2.101(14)	2.043(14)
Co–O(3b)	2.253(15)	2.145(15)	1.981(15)	1.973(15)
O(1)–Co–O(3)	89.6–104.1(6)	90.2–104.7(5)	90.8–104.6(6)	92.0–106.4(6)
O(1)–Cu–O(2)	90.5–95.5(6)	92.4–96.2(6)	93.7–95.9(6)	91.7–100.6(6)
Cu–O(1)–Co	162.2(9)	161.1(9)	161.1(9)	157.0(9)

Fig. 4. Temperature dependencies of the field-cooled (FC) and zero-field-cooled (ZFC) magnetic susceptibilities for $CoSr_2Y_{2-x}Ce_xCu_2O_{9\pm\delta}$ ($x = 0.5, 0.6, 0.7, 0.8$).

350 K at both 0 and 5 T; there was no evidence of magnetoresistance in any of the samples at any temperature. The 290 and 6 K values of resistivity increase from 0.22 to 0.68 Ω cm and from 43 to 958140 Ω cm respectively as x increases from 0.5 to 0.8. A single activated dependence of ρ with temperature could not account for the full range of the resistivity data for the $CoSr_2Y_{2-x}Ce_xCu_2O_{9\pm\delta}$ solid solutions. Variable range hopping behaviour (VRH) is observed below 100 K for all samples. The low temperature resistivity data for $CoSr_2Y_{2-x}Ce_xCu_2O_{9\pm\delta}$ ($x = 0.5, 0.6, 0.7$) can be fitted to the three dimensional Mott VRH equation [24] $\rho = \rho_0 \exp(T_0/T)^{1/4}$ (Fig 5(a)); a poor fit was obtained for the $x = 0.8$ sample using this model.

Fig. 5(b) displays the variation of $\ln(\rho)$ against $1/T^{1/2}$ for $CoSr_2Y_{1.2}Ce_{0.8}Cu_2O_{9\pm\delta}$ which is linear below $T = 100$ K. Hence the resistivity data of the $x = 0.8$ sample can be modelled by the two dimensional Efros and Shklovskii VRH model [25] $\rho = \rho_0 \exp(T_0/T)^{1/2}$; a poor fit was obtained for $x = 0.5, 0.6$ and 0.7 using this model. Above 100 K the electronic behaviour is contributed by thermally activated charge carriers across a band gap and was modelled by $\rho = \rho_0 \exp(E_g/2kT)$; the E_g values are tabulated in Table 2.

4. Discussion

The results from Rietveld refinement of the X-ray diffraction data show that there is no change in crystal structure upon increasing x in the $CoSr_2Y_{2-x}Ce_xCu_2O_{9\pm\delta}$ solid solutions. However the apical Cu–O(1) and the in-plane Cu–O(2b) bonds both expand from 2.295(9) and 1.901(4) to 2.322(9) and 1.923(4) respectively as x increases from 0.5 to 0.8; consequently the cell volume increases with x. At the same time the apical Co–O(1) and in plane Co–O(3) bonds decrease as x increases from 0.5 to 0.8 (Table 1). The observation of an increase in the average apical Cu–O bond with Ce substitution is indicative of a change in charge transfer from the Co: e_g to the Cu: $3d_{x^2-y^2}$ bands [26]. This suggests that there is a reduction of the hole concentration in the CuO$_2$ planes i.e. the oxidation state of copper is reduced as the percentage of Ce increases in the $CoSr_2Y_{2-x}Ce_xCu_2O_{9\pm\delta}$ solid solutions. This is in agreement with the electronic transport measurements; a superconducting transition is not observed for any of

Table 2
The variation of magnetic transition temperature (T_M), effective magnetic moment μ_{eff} (μ_B), Curie Weiss constant (θ), χ_0 (emu mol^{-1}), Arrhenius gap (E_g) and variable range hopping constant (T_0) with nominal x values in $CoSr_2Y_{2-x}Ce_xCu_2O_{9\pm\delta}$ as shown

x	T_M (K)	μ_{eff} (μ_B)	μ_{eff} (Co) (μ_B)	θ (K)	χ_0 (emu.mol^{-1})	E_g (eV)	T_0 (K) $\times 10^{-4}$
0.5	43(1)	5.12(2)	5.09(2)	−311 (3)	0.0002(1)	0.0263(4)	1.311(1)
0.6	48(1)	5.23(2)	5.20(2)	−344 (3)	0.0007(1)	0.0272(4)	3.940(1)
0.7	67(1)	5.29(2)	5.26(2)	−360 (3)	0.0005(1)	0.0267(4)	15.600(1)
0.8	90(1)	5.46(2)	5.43(2)	−370 (3)	0.0007(1)	0.0417(4)	1.625(1)
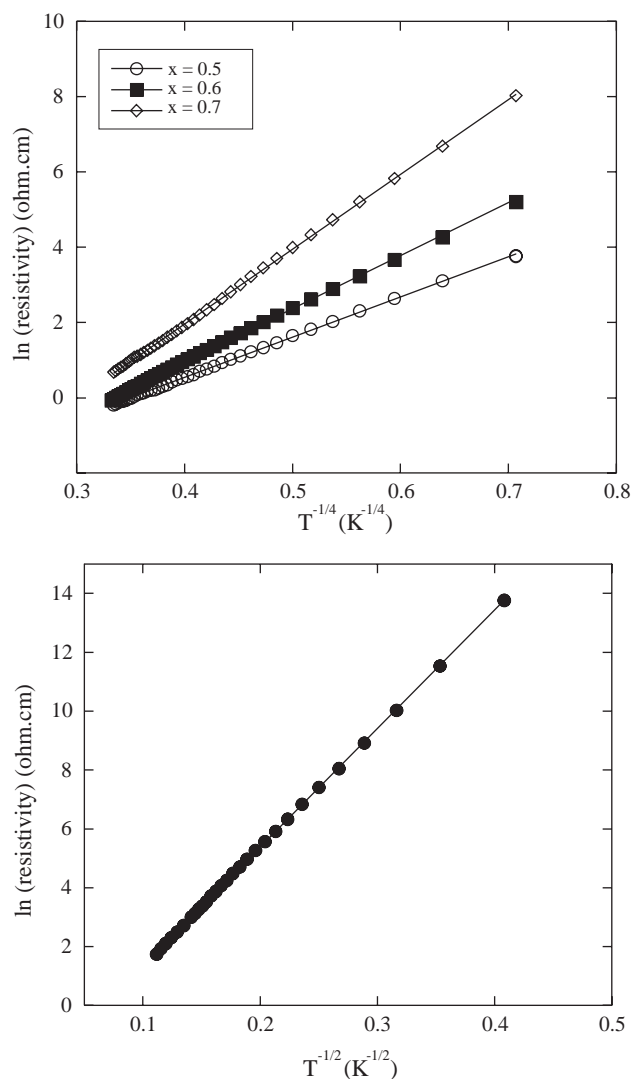
Fig. 5. Variation of ln(ρ) with (a) $T^{-1/4}$ for the $CoSr_2Y_{2-x}Ce_xCu_2O_{9\pm\delta}$ solid solutions ($x = 0.5$, 0.6, 0.7) (upper) and with (b) $T^{-1/2}$ for $CoSr_2Y_{1.2}Ce_{0.8}Cu_2O_{9\pm\delta}$ (lower).

the samples and the samples become more insulating as x increases. The oxidation state of Ce is IV in these materials [18] so that the total formal charge for (2Cu + Co) is $7.5 \pm 2\delta$ for $x = 0.5$ and $7.2 \pm 2\delta$ for $x = 0.8$ (δ is equal to the oxygen deficiency or excess in the $Y_{2-x}Ce_xO_{2\pm\delta}$ block) so that if δ is constant the total charge available decreases with x. Semiconducting

behaviour is observed for all $CoSr_2Y_{2-x}Ce_xCu_2O_{9\pm\delta}$ materials so that Cu is obviously underdoped with a valence of $\leqslant 2.05$. The low temperature resistivity data for $CoSr_2Y_{2-x}Ce_xCu_2O_{9\pm\delta}$ ($x = 0.5-0.7$) can be fitted by a Mott variable range hopping (VRH) model (Fig. 5a). T_0 is observed to rise from 1.311×10^{-4} to 15.6×10^{-4} K as x increases from 0.5 to 0.7 (Table 2) as the valence of Cu is reduced and the charge carriers become more localised. A crossover from (3D) Mott VRH to (2D) Efros Shklovskii VRH is observed for $CoSr_2Y_{1.2}Ce_{0.8}Cu_2O_{9\pm\delta}$. Efros Shklovskii VRH is observed when Coulomb correlations between localised electrons are no longer negligible and a soft Coulomb gap pinned at the Fermi level opens up. A crossover from Mott VRH to Efros Shklovskii VRH has previously been observed for $La_{2-x}Sr_xCuO_4$ at $x = 0.02$ [27] as the carrier concentration in the CuO_2 planes is reduced to a critical level. Mott VRH is observed for $La_{1.95}Sr_{0.05}CuO_4$ at low temperature and superconductivity is induced at $x = 0.055$. Hence the crossover from 3D to 2D VRH is observed as the Cu valence decreases from 2.05 to 2.02 in $La_{2-x}Sr_xCuO_4$ and so it appears that a similar reduction in the Cu valence arises in $CoSr_2Y_{2-x}Ce_xCu_2O_{9\pm\delta}$ as x increases from 0.5 to 0.8.

The apical Co–O(1) and in plane Co–O(3) bonds decrease as x increases from 0.5 to 0.8 (Table 1) which suggests that there is partial oxidation of Co^{3+} to Co^{4+} as Ce doping increases in $CoSr_2Y_{2-x}Ce_xCu_2O_{9\pm\delta}$. We previously calculated that the total formal charge for (2Cu + Co) is $7.5 \pm 2\delta$ and $7.2 \pm 2\delta$ for $x = 0.8$ (δ is equal to the oxygen deficiency or excess in the $Y_{2-x}Ce_xO_{2\pm\delta}$ block) so that if δ is constant the total charge available decreases with x. Transport measurements show that Cu is underdoped for all samples and that the valence decreases from ~ 2.05 to ~ 2.02 as x increases from 0.5 to 0.8. Hence if there are no oxygen vacancies within the $Y_{2-x}Ce_xO_{2\pm\delta}$ block the valence of Co should decrease from ~ 3.4 for $x = 0.5$ to ~ 3.16 for $x = 0.8$. Therefore a reduction in the valence of Co is expected with increasing Ce concentration if the oxygen content is kept constant. However an increase in the valence of Co is expected if an equivalent or overcompensating increase in the oxygen incorporated into the structure accompanies the extra Ce as observed in $RuSr_2Gd_{2-x}Ce_xCu_2O_{10-\delta}$ [8]. In order to investigate this further the exact oxygen stoichiometries of the

$CoSr_2Y_{2-x}Ce_xCu_2O_{9\pm\delta}$ materials were determined by thermogravimetric analysis under a 5% H_2/N_2 atmosphere. The results confirm that an overcompensating increase in the oxygen incorporated into the structure accompanies the extra Ce; as x increases from 0.5 to 0.8, δ changes from $-0.20(2)$ to $0.06(2)$. This therefore results in an increase in the oxidation state of Co from ~3 to ~3.28 as x increases from 0.5 to 0.8 in the $CoSr_2Y_{2-x}Ce_xCu_2O_{9\pm\delta}$ solid solutions.

In order to further corroborate these results, the variation of μ_{eff} with x was obtained from the Curie Weiss fit to the high temperature susceptibility data. The effective magnetic moment for cobalt was calculated by subtracting the effective magnetic moment for copper previously observed in $GaSr_2Y_{1.5}Ce_{0.5}Cu_2O_9$. ($\mu_{eff}$ (Cu) = 0.37) [28]; μ_{eff} (Co) increases from $5.09(2)\mu_B$ to $5.43(2)\mu_B$ as x increases from 0.5 to 0.8 (Table 2). Cobalt is in a tetrahedral geometry in $CoSr_2Y_{2-x}Ce_xCu_2O_{9\pm\delta}$ and is high spin (Co^{3+} e^3 t^3, Co^{4+} e^2 t^3) so that the theoretical μ_{eff} values for Co^{3+} and Co^{4+} are $4.9\mu_B$ and $5.9\mu_B$ respectively. This suggests that a small proportion of Co^{4+} may be present in $CoSr_2Y_{1.5}Ce_{0.5}Cu_2O_{9\pm\delta}$ and that this proportion increases as x rises from 0.5 to 0.8. This is in agreement with results from thermogravimetric analysis and from the variation of Co–O(1) and Co–O(3) bond lengths with increasing Ce concentration determined from Rietveld refinement of the X-ray diffraction data (Table 1). Hence it appears that the $Y_{2-x}Ce_xO_{2\pm\delta}$ block is oxygen deficient in $CoSr_2Y_{1.5}Ce_{0.5}Cu_2O_{9\pm\delta}$. As the Ce concentration increases in $CoSr_2Y_{2-x}Ce_xCu_2O_{9\pm\delta}$, extra oxygen is incorporated into the structure and charge transfer between the cuprate plane and cobaltate layer occurs so that the valence of Co increases and the valence of Cu is reduced. This is in contrast to the 1222 ruthenocuprate $RuSr_2Gd_{2-x}Ce_xCu_2O_{10-\delta}$ in which an increase in Ce doping leads to an increase in hole doping of the CuO_2 layers with no change to the oxidation state of Ru [8]. It appears that in $CoSr_2Y_{2-x}Ce_xCu_2O_{9\pm\delta}$ the extra holes induced by the overcompensating increase in oxygen incorporated into the structure accompanying Ce doping are trapped on $Co^{3+/4+}$ in the cobaltate charge reservoir. This is further corroborated by a recent study [29] of $CoSr_2(Y_{1-x}Ca_x)Cu_2O_{7+\delta}$ which has shown that as x increases Co^{3+} is oxidised preferentially to Cu^{2+}.

A magnetic transition is observed for $CoSr_2Y_{2-x}Ce_xCu_2O_{9\pm\delta}$ ($x = 0.5-0.7$) whereas low dimensional antiferromagnetism is observed for $CoSr_2Y_{1.2}Ce_{0.8}Cu_2O_{9\pm\delta}$. It has been concluded from previous studies that the magnetic order originates within the cobaltate layer [18,19,22,29]. Divergence between the zero-field cooled (ZFC) and field cooled data (FC) is observed for $x = 0.5-0.7$ (Fig. 4) at the magnetic transition which is suggestive of ferromagnetism, weak ferromagnetism (canted antiferromagnetism) or spin glass behaviour. The low temperature susceptibility is reminiscent of that

observed for the layered cobalt oxysulphide $Sr_2Cu_2CoO_2S_2$ in which 3D antiferromagnetic order between Co spins has been observed from neutron diffraction studies at the transition temperature T_N [30]. An intrinsic feature of a spin glass is deviation from a straight line and a weak hysteresis affect observed in the field dependence of the magnetisation. Hysteresis is also observed for ferromagnetic and weak ferromagnetic order whereas a linear variation of the magnetisation with field is expected for an antiferromagnetic material. The variation of magnetisation with magnetic field for $CoSr_2Y_{1.5}Ce_{0.5}Cu_2O_{9\pm\delta}$ measured at 10 K is displayed in Fig. 6. A linear variation of magnetisation with field is observed for $x = 0.5-0.8$ showing that the dominant magnetic order in antiferromagnetic. In addition the large negative Weiss constants (θ decreases from -311 ($x = 0.5$) to -370 K ($x = 0.8$)) determined from the high temperature susceptibility data are indicative of strong antiferromagnetic exchange. Furthermore antiferromagnetic correlations have previously been observed along the Co–O chains from neutron diffraction studies of the similar 1212 cobaltocuprate $YBaCu_{3-x}Co_xO_7$ [31]. It is likely that the divergence of the ZFC and FC data at T_M is due to a degree of spin glass behaviour accompanying the antiferromagnetic transition.

The intra chain Co–O distances are 2.115(14) Å and 2.253(15) Å for $CoSr_2Y_{1.5}Ce_{0.5}Cu_2O_{9\pm\delta}$ whereas the interchain distance is 3.300(14) Å. A long range magnetic transition is observed at 43 K as antiferromagnetic order occurs along and between the chains. The Curie Weiss constant, θ, is large at -311 K in comparison to the magnetic ordering temperature ($T_N = 43$ K) so that $|\theta|/T_N = 7.2$. The large negative value of θ is indicative of strong antiferromagnetic exchange, however the interchain distance is large so that
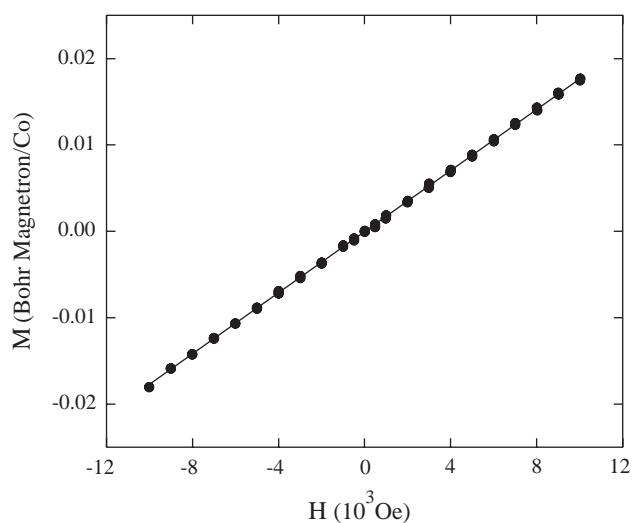

Fig. 6. Magnetic field dependence of the magnetisation of $CoSr_2Y_{1.5}Ce_{0.5}Cu_2O_{9\pm\delta}$ at 10 K.

antiferromagnetic order is only observed at low temperature. As the Ce concentration changes from 0.5 to 0.8, extra oxygen is incorporated into the structure so that Co^{3+} is partially oxidised to Co^{4+}. As a consequence the Co–O bond lengths are reduced leading to an enhancement of the superexchange interaction along the 1D chains so that the magnetic transition temperature increases from 43 to 90 K and θ decreases from -311 to -370 K. At the same time the valence of $Cu^{(2+x)+}$ is reduced (x is equal to the hole concentration in the cuprate planes) so that the overall cell volume increases leading to a flattening of the Co–O(3)–Co angle from $103.4(9)^\circ$ to $116.6(8)^\circ$. The interchain distance is observed to increase from 3.300(14) Å to 3.646(14) Å as x is varied from 0.5 to 0.8 in $CoSr_2Y_{2-x}Ce_xCu_2O_{9\pm\delta}$ so that the magnetic transition broadens and by $x = 0.8$ long range magnetic order is not observed between the chains down to 10 K and susceptibility results show behaviour analogous to a low dimensional antiferromagnet. Hence the increase in charge transfer between the cuprate and cobaltate layers with x ultimately results in the disruption of the long range magnetic order between the Co chains as the cell volume increases and the interchain distance reaches a critical length.

5. Conclusion

In conclusion we have observed antiferromagnetic order between Co spins in $CoSr_2Y_{2-x}Ce_xCu_2O_{9\pm\delta}$ ($x = 0.5-0.8$) at low temperature; a degree of spin glass behaviour accompanies the magnetic transition for $x = 0.5-0.7$. The $Y_{2-x}Ce_xO_{2\pm\delta}$ block is oxygen deficient in $CoSr_2Y_{1.5}Ce_{0.5}Cu_2O_{9\pm\delta}$ but extra oxygen is incorporated into the structure as x increases in the $CoSr_2Y_{2-x}Ce_xCu_2O_{9\pm\delta}$ solid solutions so that Co^{3+} is partially oxidised to Co^{4+}. This results in a reduction of the Co–O(1) and Co–O(3) bond lengths so that the superexchange interaction is enhanced and T_M increases from 43 to 90 K. Moreover as x increases holes are drained from $Cu^{(2+x)+}$ and as a consequence the cell volume increases so that the Co–O(3)–Co interchain bond length expands and the dimensionality of the magnetic order changes at $x = 0.8$. At the same time there is a crossover in the electronic transport from Mott VRH to Efros Shklovskii VRH at low temperature. It is intriguing that the dimension of the electronic transport and magnetic order changes simultaneously as x increases from 0.7 to 0.8 and suggests that the cobaltate layers may be involved in charge transport in addition to the CuO_2 planes. However a crossover from Mott VRH to Efros Shklovskii VRH has previously been observed as the charge carriers are reduced in the lightly doped cuprates. Neutron diffraction studies are currently underway to determine the magnetic structure of $CoSr_2Y_{2-x}Ce_xCu_2O_{9\pm\delta}$ and to study the exact variation of δ with x.

Appendix A. Supplementary data

The online version of this article contains additional supplementary data. Please visit doi:10.1016/j.jssc.2004.08.007.

References

[1] L. Bauernfeind, W. Widder, H.F. Braun, Physica C 254 (1995) 151.
[2] I. Felner, U. Asaf, Y. Levi, O. Millo, Phys. Rev. B 55 (1997) 3374.
[3] C. Bernhard, J.L. Tallon, C. Niedermayer, T. Blasius, A. Golnik, E. Brucher, R.K. Kremer, D.R. Noakes, C.E. Stronach, E.J. Ansaldo, Phys. Rev. B 59 (1999) 14099.
[4] A.C. Mclaughlin, W. Zhou, J.P. Attfield, A.N. Fitch, J.L. Tallon, Phys. Rev. B 60 (1999) 7512.
[5] O. Chmaissam, J.D. Jorgensen, H. Shaked, P. Dollar, J.L. Tallon, Phys. Rev. B 61 (2000) 6401.
[6] J.W. Lynn, B. Keimer, C. Ulrich, C. Bernhard, J.L. Tallon, Phys. Rev. B 61 (2000) R14964.
[7] C.S. Knee, B.D. Rainford, M.T. Weller, J. Mater. Chem. 10 (2000) 2445.
[8] A.C. Mclaughlin, J.P. Attfield, U. Asaf, I. Felner, Phys. Rev. B 68 (2003) 014503.
[9] W.E. Pickett, R. Weht, A.B. Shick, Phys. Rev. Lett. 62 (1999) 4132.
[10] C. Bernhard, J.L. Tallon, E. Brucher, R.K. Kremer, Phys. Rev. B 61 (2000) 14960.
[11] Y.Y. Xue, S. Tsui, J. Cmaidalka, R.L. Meng, B. Lorenz, C.W. Chu, Physica C 341 (2000) 483.
[12] I. Dzyaloshinksy, Sov. Phys. JETP 5 (1957) 1259.
[13] T. Moriya, Phys. Rev. 120 (1960) 91.
[14] K. Yamaura, D.P. Young, R.J. Cava, Phys. Rev. B 63 (2001) 064401.
[15] G. Briceño, H. Chang, X. Sun, P.G. Schulz, X.-D. Ziang, Science 270 (1995) 273.
[16] C. Martin, A. Maignan, D. Pelloquin, N. Nguyen, B. Raveau, Appl. Phys. Lett. 71 (1997) 1421.
[17] A.J. Wright, C. Greaves, Physica C 235 (1994) 885.
[18] M. Karppinen, V.P.S. Awana, Y. Morita, H. Yamauchi, Physica C 392–396 (2003) 82.
[19] V.P.S. Awana, A. Gupta, H. Kishan, S.K. Malik, W.B. Yelon, J. Linden, M. Karppinen, H. Yamauchi, D.C. Kundaliya, J. Appl. Phys. 95 (2004) 6690.
[20] H.M. Rietveld, Acta Cryst. 22 (1967) 151.
[21] A.C. Larson, R.B. Von Dreele, Los Alamos National Laboratory Report No. LA-UR-86-748, 1994.
[22] X.G. Luo, X.H. Chen, X. Liu, R.T. Wang, Y.M. Xiong, C.H. Wang, G.Y. Wang, X.G. Qiu, Phys. Rev. B 70 (2004) 054520.
[23] M. Matoba, T. Takeuchi, S. Okada, Y. Kamihara, M. Itoh, K. Ohoyama, Y. Yamaguchi, Physica B 312 (2002) 630.
[24] N.F. Mott, Metal-Insulator Transitions, Taylor & Francis, London, 1974.
[25] A.L. Efros, B.I. Shklovskii, J. Phys. C 8 (1975) L49.

[26] R.J. Cava, A.W. Hewat, E.A. Hewat, B.A. Batlogg, M. Marezio, K.M. Rabe, J.J. Krajewski, W.F. Peck Jr., L.W. Rupp Jr., Physica C 165 (1990) 419.

[27] B. Ellman, H.M. Jaeger, D.P. Katz, T.F. Rosenbaum, A.S. Cooper, G.P.E. Spinosa, Phys. Rev. B 39 (1989) 9012.

[28] L. Rukang, R.K. Kremer, J. Maier, Physica C 200 (1992) 344.

[29] Y. Morita, H. Yamauchi, M. Karppinen, Solid State Commun. 127 (2003) 493.

[30] S. Okada, M. Matoba, H. Yoshida, K. Ohoyama, Y. Yamaguchi, J. Phys. Chem. Solids 63 (2002) 983.

[31] F. Maury, I. Mirebeau, J.A. Hodges, P. Bourges, Y. Sidis, A. Forget, Phys. Rev. B 69 (2004) 094506.